Extensive Phylogeographic and Morphological Diversity in *Diporiphora nobbi* (Agamidae) Leads to a Taxonomic Review and a New Species Description

Extensive Phylogeographic and Morphological Diversity in *Diporiphora nobbi* (Agamidae) Leads to a Taxonomic Review and a New Species Description

Danielle L. Edwards[1] and Jane Melville

Department of Sciences, GPO Box 666, Museum Victoria, Melbourne, VIC 3001, Australia

Abstract.—Morphological and molecular information is invaluable in the description of cryptic diversity and the evolutionary processes driving diversification within closely related species that exhibit morphological homoplasy. We present a distribution-wide data set consisting of both molecular and morphological information, providing a taxonomic revision of the *Diporiphora nobbi* species group, and develop preliminary hypotheses regarding the evolutionary history of *D. nobbi*. We show deep molecular divergence between *D. nobbi* and a newly described sister lineage associated with divergence in meristic characters. Our molecular data also show large divergences among subclades within nominate *D. nobbi* associated with different habitats rather than specific biogeographc barriers. We further discuss potential diversification mechanisms within the *D. nobbi* species group.

Integration of morphological and molecular data has become a powerful tool for resolving taxonomic issues, diversification mechanisms, and biogeographic pattens, particularly for groups with traditionally uncertain or difficult taxonomic reconstruction. The Australian agamid lizards are one such group where both higher level, inter- and intrageneric taxonomic relationships have been difficult to resolve due to a lack of diagnostic morphological characters and high levels of intraspecific phenotypic variation. Molecular techniques have proven invaluable in resolving the higher level systematics of the group (Macey et al., 2000; Schulte et al., 2003; Hugall and Lee, 2004; Hugall et al., 2008) that remained uncertain under a purely morphological framework. Molecular studies also have shown that the Australian agamids form a single evolutionary lineage (Macey et al., 2000), known as the subfamily Amphibolurinae, that diversified across Australia's arid and semiarid regions during the Miocene in response to an increasingly dry environment (Hugall et al., 2008).

More recent intrageneric molecular work has demonstrated that there is great variation in the level of morphological diversity within evolutionary lineages of the Amphibolurinae. One well-studied genus within Amphibolurinae, *Ctenophorus*, has shown dramatic diversity in morphological evolution between closely related species (Melville et al., 2001). However, the opposite has been found in other genera, with widespread "species" being found to be cryptic species complexes (Melville et al., 2008; Shoo et al., 2008), some of which display morphological stasis rather than disparity (Smith et al., 2011). Such variation in the level of morphological diversity within lineages reinforces the importance of integrating molecular and morphological data when undertaking taxonomic reviews in the Australian agamid lizards.

Diporiphora is one of the more species-rich genera within Amphibolurinae and contains many lineages for which taxonomic revision is needed. *Diporiphora nobbi*, a recent addition to this genus after molecular revision (Schulte et al., 2003; Hugall and Lee, 2004; Hugall et al., 2008), has a distribution that encompasses the majority of eastern Australia. The huge distribution and the extensive morphological variation seen in this species suggest that an investigation of its phylogeographic variation and a taxonomic review is warranted.

Witten (1972) originally described *D. nobbi* as a member of the *Amphibolurus muricatus* species group from material collected across New South Wales (NSW) and southeastern Queensland (QLD), assigning the species name *Amphibolurus nobbi*. Although affinities between *A. nobbi* and *Diporiphora* were not directly analyzed in the original description of the species by Witten (1972), Witten did in fact note the "superficial resemblance" between *A. nobbi* and *Diporiphora*. However, Witten (1972) considered *Amphibolurus muricatus* the sister species to the new taxon based on the presence of femoral pores in *A. nobbi*, which are generally not present in *Diporiphora* species. Later, Greer (1989) noted that color patterns in *A. nobbi* were similar to those of other species of *Diporiphora*, rather than to *Amphibolurus*, with a pink or rose flush to the base of the tail and yellowish sides. Molecular analyses have since revised the taxonomy of the species to show that *A. nobbi* was in fact nested within *Diporiphora* (Schulte et al., 2003; Hugall and Lee, 2004; Hugall et al., 2008). These molecular analyses have included multiple loci of both mitochondrial DNA (mtDNA) and nuclear DNA and are supported by several phylogenetic studies undertaken on Amphibolurinae in recent times (Schulte et al., 2003; Hugall and Lee, 2004; Hugall et al., 2008). Thus, we refer to this species as *D. nobbi*.

There are currently two described subspecies within *D. nobbi*, *D. n. nobbi* and *D. n. coggeri*, both described from the cool temperate forests and upland areas of the New England Tablelands (Fig. 1). Wells and Wellington (1985) described another species from within the range of *D. nobbi* and ascribed this species to its own genus with the name *Wittenagama parnabyi* based on a single specimen from central Queensland in the vicinity of Alpha. However, this species was later synonymized with *D. nobbi* by Shea and Sadlier (1999).

The distribution of *D. nobbi* covers steep environmental and ecological gradients, from rain forest, dry woodlands, and coastal swamplands and vegetation to cool temperate forests and upland areas, as well as dry mallee with spinifex woodland. This distribution also crosses many important biogeographic barriers known to delineate population structure in its sister lineage *D. australis* (Edwards and Melville, 2010) and many other woodand, highland, and rain forest species throughout QLD and NSW (Schneider et al., 1998; Moritz et al., 2000; Dolman and Moritz, 2006; Moussalli et al., 2009). *Diporiphora nobbi* shows a large amount of geographic variation in body size, morphology, and male secondary sexual coloration at the tail base (e.g., often displaying a purple, pink, or red flush; Cogger, 2000), with some forms showing stark body coloration (e.g., the Alpha form having a canary yellow body in displaying males; pers. obs.).

To clarify the taxonomic status of *D. nobbi*, we compiled a multilocus molecular data set in combination with morphological data collected from museum voucher specimens from across the distribution. Specifically, we sought to test whether *D. n. nobbi*, *D. n. coggeri* (Witten, 1972), and *W. parnabyi* (Wells

―――――――――
[1] Corresponding Author. Present address: 119A Environmental Science Center, Department of Ecology and Evolutionary Biology, Yale University, New Haven, CT 06520-8106 USA. E-mail: Dan.Edwards@yale.edu
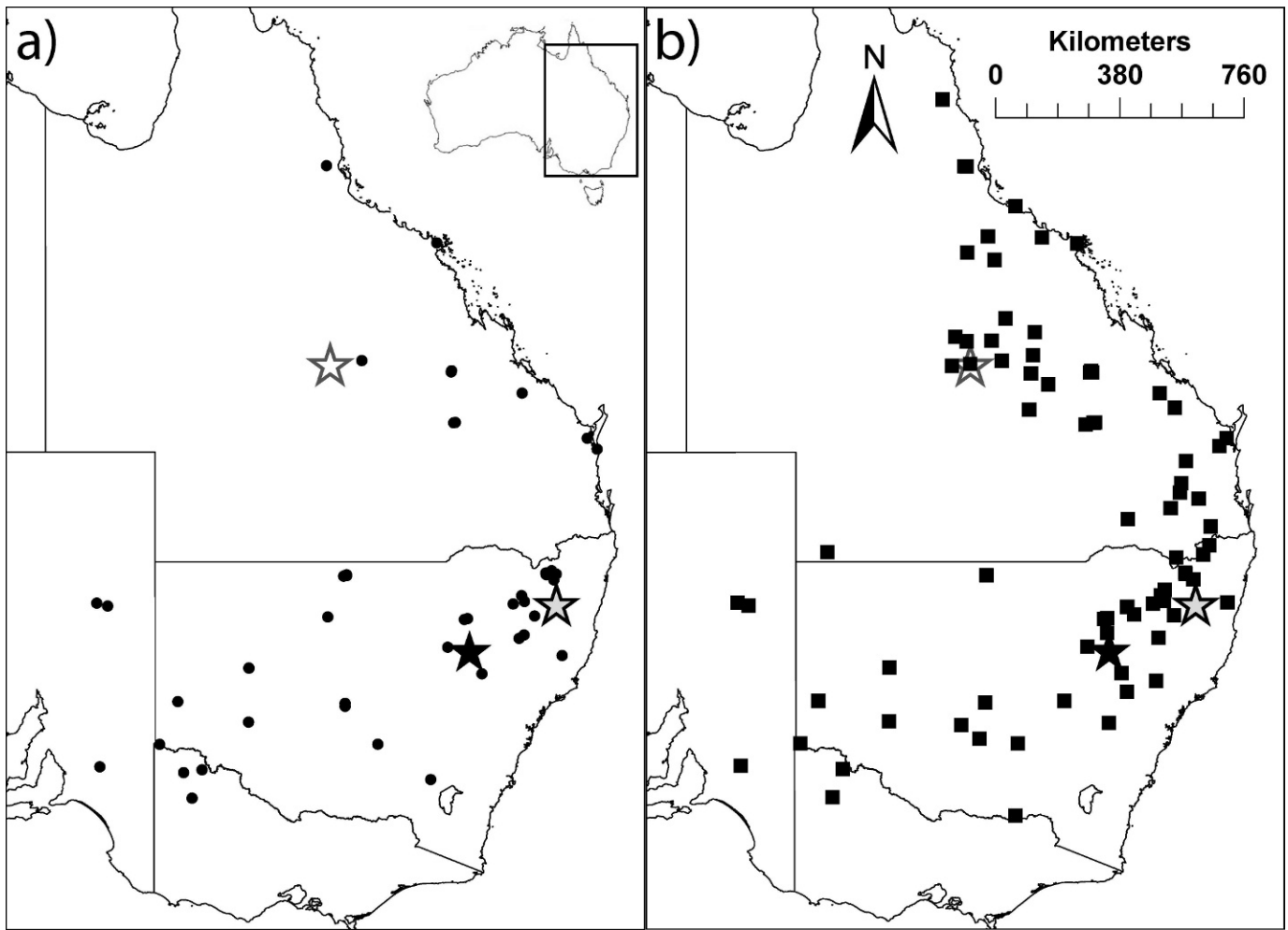
FIG. 1. Map of sampling locations for tissues used for genetic analysis (a, ●) and material examined for morphological analyses (b, ■). The type localities for each of the nominate subspecies within *Diporiphora nobbi* are shown (*D. n. nobbi*, open black and gray star; *D. n. coggeri*, solid black star), as is the type locality for the previously synonymized *Wittenagama parnabyi* (open gray and white star). Map of Australia is inset.

and Wellington, 1985) could be ascribed species status. Providing a complete assessment of molecular and morphological variation in *D. nobbi*, we contribute an important advance in our understanding of the biogeographic history and taxonomy of eastern Australian vertebrate fauna.

MATERIALS AND METHODS

Taxonomic Sampling.—Sampling effort focused on gathering tissue samples from across the distributions of both nominate subspecies in the *D. nobbi* species group—*D. n. nobbi* and *D. n. coggeri*. This was accomplished using a combination of tissues deposited in Australian museums and fresh tissue collections. In total, 90 individuals were sampled from across the species distribution, including the distributions of both nominal subspecies, with one to five animals per site (Fig. 1a; for details on each sample, see Appendix 1). For fresh field collections two specimens per site were deposited in the Museum Victoria Collection (liver tissue); the remaining animals from each site were nonlethally sampled (tail-tips) and released at the point of capture. Specimens and tissues collected fresh have been listed in Appendix 1 (MVD and MVZ numbers).

Museum samples were obtained from the Australian Museum Tissue Collection, Australian Biological Tissue Collection (South Australian Museum), and the Queensland Museum Tissue Collection. Morphological measurements were

taken from all suitable specimens for which molecular data were available. In addition, to encompass the morphological variation across the group and determine appropriate species assignment, specimens representing gaps in tissue collections and potential species boundaries were morphologically measured in conjunction with holotypes or paratypes (For distribution of material examined, see Fig. 1b; for details of material examined, see Appendix 2). Paratypes were included for both nominal subspecies within the *D. nobbi* species complex (*D. n. nobbi* and *D. n. coggeri*) in addition to the holotype for *W. parnabyi* (Wells and Wellington, 1985), which was synonymized with *D. nobbi* by Shea and Sadlier (1999).

Outgroup samples for mtDNA analyses were selected from across *Diporiphora* and associated genera (*D. australis*, GU556007; *D. bilineata*, AF128473; *A. nobbi*, AY132999; *D. albilabris*, AY133003; *D. arnhemenica*, AY133004; *Caimanops amphiboluroides*, AF128472; *D. magna*, AY133009; *D. winneckii*, AY133012; and *A. muricatus*, AF128468). For specific information on each of these *ND2* sequences, refer to Melville et al. (2001), Schulte et al. (2003), and Edwards and Melville (2010). For recombination activating gene-1 (*RAG1*) analyses, outgroups were obtained from previously published sequences from across *Diporiphora* and associated genera (Appendix 3). In addition, sequence data were obtained for *D. australis* (MVD74106; vicinity of Charters Towers [20° 12′ 57.2″E 146° 14′ 43.4″S]; GenBank # JN815263) for *RAG1* to supplement these sequence data.

Molecular Data.—Genomic DNA was extracted from the tail and liver samples by using a modified chloroform method, suspended in Tris-EDTA buffer, and stored at $-20°C$ (for details, see Shoo et al., 2008). For all individuals, we targeted an ~1,400-bp fragment of mtDNA incorporating the entire protein-coding gene NADH dehydrogenase subunit 2 (*ND2*) and the genes encoding tRNA[Trp], tRNA[Ala], tRNA[Asn], tRNA[Cys], and tRNA[Tyr] to the beginning of the protein-coding gene subunit I of cytochrome *c* oxidase. For a subset of these animals, we sequenced an ~1,400-bp fragment of nuclear DNA incorporating a portion of the *RAG1* exon to ensure resulting relationships could be confirmed across multiple mtDNA and nuclear loci.

Targeted DNA was amplified using a touch-down polymerase chain reaction (PCR) profile (94°C for 5 min, 1×; 94°C for 30 sec, 70–45°C (decreasing in 5°C increments) for 20 sec, 72°C for 90 sec, 2×; 94°C for 30 sec, 40°C for 30 sec, 72°C for 45 sec, 40×; 72°C for 4 min, 1×; 4°C, hold. Primers used to amplify *ND2* were Metf-1 (5′-AAGCAGTTGGGCCCATRCC-3′, complement of H4419b) (Macey et al., 2000) and H5934 (5′-AGRGTGCCAATGTCTTTGTGRTT-3′) (Macey et al., 1997) or CO1r.aga (5′-ACRGTTCCRATRTCTTTRTGRTT-3′) (Macey et al., 2000). Primers used to amplify *RAG1* were JRAG1f.1 (5′-CAAAGTGAGACSACTTGGAAAGCC-3′) and JRAG1r.13 (5′-CATTTTTCAAGGGTGGTTTCCACTC-3′) (Shoo et al., 2008). Targeted fragments were amplified in 40-μl reactions consisting of ~100 ng of template DNA, 4 μl of 10× reaction buffer, 3 mM MgCl₂, 0.5 mM dNTPs, 10 pmol of each primer, and 2 units HotStart *Taq* polymerase (MBI Fermentas). PCR products were purified using a SureClean PCR cleanup kit (Bioline) or gel purified using GFX columns (GE Healthcare) and then sent to Macrogen Inc. (Seoul, Korea) for sequencing. Internal primers *ND2*f.17 (5′-TGACAAAAAATTGCNCC-3′) (Macey et al., 2000) and *ND2*f.dip (5′-AAATRATAGCCTACTCAT-3′) (Shoo et al., 2008) were used in addition to PCR primers to obtain reliable sequence across the *ND2* gene. DNA sequence data were then edited using Sequencher 4.1.4 (Gene Codes Corporation). Sequences were aligned individually using ClustalX (Thompson et al., 1997). Alignments were then checked by eye. Protein coding regions were translated using the mammalian genetic code option in Sequencher 4.1.4 (Gene Codes Corporation), and a clear reading frame was observed in all *ND2* sequences. Thus, sequences were assumed to be genuine mitochondrial copies and not nuclear paralogs. Sequences have been lodged in GenBank (Appendix 1).

Phylogenetic Analyses.—Bayesian and maximum likelihood (ML) analyses of haplotype sequences were used to assess overall phylogenetic structure and support for major clades in Mr Bayes version 3.1.2 (Ronquist and Huelsenbeck, 2003) and RAxML (Stamatakis et al., 2008) individually for both *ND2* and *RAG1* data sets. Modeltest 3.7 (Posada and Crandall, 1998), using Akaike information criterion showed that for the mtDNA data the GTR + I + Γ model of nucleotide substitution best fit the data, and for the *RAG1* data the TRN + I + Γ model of nucleotide substitution best fit the data. Bayesian and ML analyses were conducted using these best fit models of nucleotide substitution and partitioned according to codon position for mtDNA data. Bayesian analyses were undertaken using default priors for Markov chain Monte Carlo analyses in MrBayes version 3.1.2 (Ronquist and Huelsenbeck, 2003). Bayesian analyses consisted of four independent runs of four chains each, sampling every 100 generations run for 10×10^6 generations for the *ND2* data set and for 4×10^6 generations for the *RAG1* data set to ensure convergence. Burn-in was set at 1,000,000 and 400,000 generations for the *ND2* and *RAG1* analyses, respectively. Convergence of posterior probabilities and stationarity of likelihood scores between the runs were assessed in Tracer version 1.4 (Rambaut and Drummond, 2005). ML analyses were run for 100 bootstrap replicates.

Estimates of Divergence Times.—We estimated divergence times for both the *ND2* and *RAG1* data sets separately using the relaxed molecular clock method in the program BEAST version 1.6.1 (Drummond and Rambaut, 2007). Initial analyses used several fossil calibrations across Reptilia, and specifically within the Iguania, we used an expanded dating data set as per Shoo et al. (2008) and Melville et al. (2009), sampling across the Reptilia by using GenBank sequences (for outgroups used and their associated accessions, see BEAST output in Appendix 4). Given the issues regarding overestimated divergences caused by saturation-driven branch length truncation (Hugall et al., 2007; Sanders et al., 2008), *RAG1* and mtDNA analyses were run separately. Analysis of the *RAG1* data set used fossil calibrations across the Iguania to estimate the divergence between *D. nobbi* and *D.* sp. nov. Fossil calibrations included four fossils used in previously published studies: a middle Jurasic acrodont iguanian fossil (154–180 mya, Evans et al., 2002), an early Miocene sceloporine (~22.8 mya , Robinson and Van Devender, 1973) and an *Chamaeleo/Rhampholeon* fossil (18 mya, Rieppel et al., 1992), and a Pliocene *Phrynocephalus* fossil (5 mya, Zerova and Chkhikvadze, 1984). Specific BEAST settings for these calibrations are as per table 1 in Melville et al. (2009). In addition, we added a minimum age estimate for the *Physignathus lesueurii* lineage (which includes that majority of the Australian amphibolurine species, except *Moloch*, *Chelosania*, and *Hypsilurus*) of 20 mya (Covacevich et al., 1990) with BEAST settings as follows: mean = 1.8, SD = 1.0, and zero offset = 20. The Iguania and Episquamata were held as monophyletic and all other relationships were free to vary.

Given the difficulties in resolving the intraspecific clade relationships within nominate *D. nobbi* by using the *RAG1* data and considering the difficulties with using deep calibrations with mtDNA as mentioned above, we used a reduced sampling approach to estimate divergence times of phylogeographic clades. For the mtDNA analysis, we used only the *Phrynocephalus* and *P. lesueuri* fossil calibrations using the BEAST settings described above and in Melville et al. (2009). All relationships were allowed to vary.

Both mtDNA and nuclear analyses employed a GTR + I + Γ model of evolution, by using an uncorrelated lognormal relaxed molecular clock. A Yule Speciation Process tree prior also was used for both analyses. *RAG1* analyses were run for 15 million generations and mtDNA analyses were run for 10 million generations with burnins of 150,000 and 100,000, respectively. All fossils are a minimum estimate of age; therefore, we used lognormal distribution for fossil calibrations. Output files were reviewed in Tracer version 1.4 (Rambaut and Drummond, 2005) to check that stationarity had been reached, to examine the coefficient of variation, to determine the appropriateness of a lognormal clock, and to assess the autocorrelation of rates from ancestral to descendant lineages (Drummond et al., 2006).

Morphological Data and Analyses.—Both morphometric and meristic character counts were taken from 113 specimens from across the range of *D. nobbi* (Fig. 1b), incorporating both specimens with and without molecular data, holotypes of described subspecies, and previously synonymized species holotypes. Thirteen morphometric measurements were obtained: snout–vent length (SVL), axillo–groin length (AG), head length (HL), snout length (SL), head depth (HD), head width (HW), nostril width (NW), interorbital width (IOW), arm length (ArL), metacarpal length (McL), leg length (LgL), metatarsal length (MtL), and tail length (TaL). Twenty-six meristic characters, both continuous and categorical, also were measured for all specimens. Continuous characters included the following: right and left femoral pore number (RFP & LFP), right and left preanal pore number (RPP & LPP), number of lamellae on Finger IV (McL), number of lamellae on Toe IV (MtL), number of infralabial scales (ILS), number of supralabial

scales (SLS), tympanum width (TyW), postauricular spine number (PAS), upper auricular spine number (UAS), secondary upper auricular spine number (SAUS), nuchal spine number (NS), scapular spine number (SS). Categorical characters included the following: strength of gular fold (SGF), strength of scapular fold (SSF), strength of paravertebral scale keeling (PVS), regularity of paravertebral scale keeling (RPVS), regularity of scales between PV rows (RBwPVS), nuchal spine position (NSP), dorsolateral spines (DLS), throat color (TC), dorso-lateral body color (DLC), and lip-scale color (LC). Refer to Table 1 for details on categories and units and on methods of measurement for each character.

Only adult specimens (>50 mm SVL) were measured to avoid ontogenetic changes in morphological measurements, and male ($N = 64$) and female ($N = 49$) animals were analyzed separately to avoid problems associated with sexual dimorphism. Averages and SEM for each measurement are presented in Table 2. We sought to differentiate species based on the putative species to which they belonged (i.e., *D. nobbi*, $N = 55$ males and $N = 42$ females versus *D.* sp. nov., $N = 9$ males and $N = 7$ females). There was not enough data to distinguish whether genetic clades within *D. nobbi* differed substantially, because specimens available for both morphological and genetic analysis were limited. Morphometric and meristic data sets were analyzed separately. All morphometric measurements were log-transformed to ensure normality and then regressed against SVL to remove any allometric effects of body size. The residuals were then plotted against SVL to ensure the effects of body size had been removed; these residuals were then used for subsequent analyses. Continuous morphometric variables were regressed against SVL to adjust for differences in body size, and the residuals of these values were used in subsequent analyses.

Principal components analyses (PCAs) were used to determine the relevance of morphometric measurements and meristic characters, respectively, in MYSTAT version 12 (Systat Software Inc., Chicago, IL, USA). Initial PCAs were undertaken to identify those variables that best diagnosed the two species of *Diporiphora* (i.e., as indicated by high eigenvalues in the PCA), these variables were used as an optimal set for further analyses. The number of principal components (PCs) extracted from the analysis was determined from a scree-plot analysis of eigenvalues. Individuals were then grouped into species, and their individual factor scores were plotted in Euclidean space. Paired *t*-tests were used to test for divergence in morphometric factor scores and meristic dimension scores between species. A Bonferroni post-hoc test identified whether the two species significantly differed in PC scores.

Results

Phylogenetic Analyses.—Mitochondrial sequencing from 90 individuals yielded 60 *ND2* haplotypes for a 1,378-bp fragment including the entire protein coding gene *ND2*, with 376 variable sites of which 317 were parsimony informative. Total nucleotide diversity (π) for the whole mtDNA data set was 0.05710, with $\pi = 0.02615$ and 0.04993 for the two major clades associated with *D. nobbi* and *D.* sp. nov., respectively. A subset of 24 individuals was selected from the sequenced mtDNA individuals for nuclear phylogenetic analyses. Across these 24 individual sequences for the 1,367-bp fragment of *RAG1* 157 bp was variable, 64 of which were parsimony informative, with $\pi = 0.0032$ across the entire data set. Twenty of these sequences contained at least one heterozygous site; these ambiguous sites were coded using standard International Union of Pure and Applied Chemistry codes.

Phylogenetic analyses of the mtDNA data uncovered two major clades within *D. nobbi*. The first of these major clades was associated with *D. nobbi* as a whole and contained a large amount of genetic diversity, including six subclades broadly associated with distinct geographic regions (Fig. 2). Animals associated with the central NSW woodlands, western NSW slopes and highland forests, Murray River basin mallee–spinifex woodlands, north coastal QLD forests, and central western QLD woodlands formed distinct clades within a monophyletic group encompassing the majority of the known range of *D. nobbi*. Relationships among the subclades within this group were not able to be resolved using the mtDNA data set. Reciprocally monophyletic and sister to this group was a group of animals occurring within southeastern QLD and coastal northern NSW.

The second major clade was associated with a previously unidentified cryptic species from the Carnarvon Gorge area in central western QLD. The specific relationships between this new species, *D. nobbi*, and *D. australis–D. bilineata* were uncertain given the mtDNA data set, and although separate from other *Diporiphora* species included in the phylogeny, were not well supported as a distinct species group (Fig. 2). However, *D. nobbi* and the previously undescribed species were clearly nested within *Diporiphora* as per the results of all previous molecular studies.

Phylogenetic analyses undertaken with the *RAG1* (Fig. 3) data set could not resolve relationships among the distinct subclades within *D. nobbi*. However, there was strong support for the reciprocally monophyletic sister relationship between *D. nobbi* and *D.* sp. nov. There was also strong support for the *D. australis* species group as a sister to the *D. nobbi* species complex. These data also support *D. nobbi* as a member of *Diporiphora*.

Divergence Analyses.—The relaxed lognormal clock analysis of the mtDNA data set (Appendix 4) produced the same ingroup topology as the phylogenetic analyses (Fig. 2). For both the *RAG1* and mtDNA analyses, there was a slight tendency toward a positive correlation in the rate of parent to child branches, with a covariance of -0.0121 and 0.0588, respectively. However, because the 95% highest posterior distribution (HPD; -0.17 to 0.15 and -0.1 to 0.23, respectively) included zero, this autocorrelation was not considered significant (Drummond et al., 2006). The coefficient of rate variation was estimated to be 0.45 (95% HPD, 0.36–0.55) and 0.51 (95% HPD, 0.41–0.62 95%) for the *RAG1* and mtDNA data sets, respectively, indicating that neither data set is strictly clock-like and that a lognormal relaxed clock is appropriate. The complete BEAST output trees are supplied in Appendices 3 and 4, showing the nuclear and mtDNA data sets, respectively.

Our divergence analyses (Figs. 2, 3) produced an age for Amphibolurinae (including *Physignathus cocincinus* and all other Australasian agamids) at 40.37 mya (95% HPD, 28.3–54.2 mya) for the *RAG1* data and 30.48 mya (95% HPD, 22.9–39.9 mya) for the mtDNA data. Our *RAG1* divergence estimates are slightly elevated with broader confidence limits compared with those reported previously for the age of Amphibolurinae by using much larger data sets (Hugall and Lee, 2004; Hugall et al. 2008); however, our confidence limits still overlap within the ranges reported in these more comprehensive studies, and some discrepancy is to be expected considering the use of a point estimate calibration as opposed to the distribution of ages used in our study. Our divergence estimates for the purely Australasian Amphibolurinae (including *Moloch*, *Hypsilurus*, and all remaining Australian agamid genera) are 29.2 mya (95% HPD, 21.6–37.7 mya) for the *RAG1* data and 24.1 mya (95% HPD, 20.2–30.2 mya) for the mtDNA data, again overlapping with previously published data (Hugall and Lee, 2004; Hugall et al. 2008).

Our estimates of divergence (Figs. 2, 3) suggest the age of the *Diporiphora australis–D. nobbi* lineage is ~10 mya (95% HPD for *RAG1*, 13.2 mya [7.7–19.2 mya]; 95% HPD for mtDNA, 10.7 mya

TABLE 1. Morphological and morphometric characters measured for specimens of *Diporiphora nobbi*. Included is a detailed description of each measurement, the abbreviation used and the type, units, or categories used to classify each measurement. DL, dorso-lateral; PAF, postauricular fold; PV, paravertebral.

Type of character	Character name	Abbreviation	Method of measurement	Unit/category/type
Morphometric characters	Snout–vent length	SVL	Distance between the tip of the nose and the cloaca	Millimeters
	Axillo–groin length	AG	Distance between the posterior of the forelimbs and the anterior of the hind limbs	Millimeters
	Snout length	SL	Distance between the anterior orbital cavity and the tip of the nose	Millimeters
	Head length	HL	Distance between the tip of the nose and the base of the skull	Millimeters
	Nose width	NW	Width of the skull between the nostrils	Millimeters
	Interorbital width	IOW	Width of the skull between the occular ridges	Millimeters
	Head width	HW	Width of the skull at its widest point between the occular cavity and the base of the skull	Millimeters
	Arm length	ArL	Length of the arm from the tip of the claw on the 4th digit to where the arm joins the body	Millimeters
	Leg length	LgL	Length of the leg from the tip of the claw on the 4th digit to where the leg joins the body	Millimeters
	Metacarpal length	McL	Distance from tip of the fourth digit to the attachment to the hand	Millimeters
	Metatarsal length	MtL	Distance from the tip of the fourth digit to the attachment to the foot	Millimeters
Meristic characters (continuous)	Right femoral pores	RFP	No. of femoral pores on the right leg	Count
	Left femoral pores	LFP	No. of femoral pores on the left leg	Count
	Right preanal pores	RPAP	No. of preanal pores on the right side anterior to the cloaca	Count
	Left preanal pores	LPAP	No. of preanal pores on the left side anterior to the cloaca	Count
	Finger IV lamellae	McL	No. of lamellae on the forth digit on the hand	Count
	Toe IV lamellae	MtL	No. of lamellae on the forth digit on the foot	Count
	Infralabial scales	ILS	No. of scales on the upper lip	Count
	Supralabial scales	SLS	No. of scales on the lower lip	Count
	Tympanum width	TyW	Horizontal diameter of the tympanum	Millimeters
	Postauricular spines	PAS	No. of spines immediately anterior to the tympanum	Count
	Upper auricular spines	UAS	No. of spines immediately above the tympanum	Count
	Secondary upper auricular spines	SUAS	No. of spines immediately above the UAS	Count
	Scapular spines	SS	No. of scapular spines	Count
	Nuchal spines	NS	No. of nuchal spines	Count
Meristic characters (categorical)	Gular fold	SGF	Strength of gular fold	Absent/weak/strong/very strong
	Scapular fold	SSF	Strength and length of scapular fold	Absent/ weak before PV rows/ weak to PV rows/ strong before PV rows/ strong to PV rows/ strong curves over arm
	Paravertebral keeling (strength)	PVS	Strength of paravertebral scale keeling	Weak/moderate/strong
	Paravertebral keeling (regularity)	RPVS	Regularity of PV scale keeling	Even/uneven/uneven with two rows
	Scales between PV rows	SBwPVS	Regularity of scales between PV rows (outer and inner rows)	Both regular/outer row irregular, inner row moderately regular/both moderately regular/both highly irregular
	Nuchal spines (position)	NSP	Position and arrangement of nuchal spines	Absent/diagonal up from PAF no clusters/diagonal up from PAF with clusters/extend from DL PV scale row/random
	Dorso-lateral spines	DLS	Presence/absence of DL spines and their arrangement	Absent/absent but some enlarged scales/present without clusters/ present with clusters

Table 1. Continued.

Type of character	Character name	Abbreviation	Method of measurement	Unit/category/type
	Throat color	TC	Color of scales on the throat	Absent/mottling grey/mottling black/black with white chevron/black in gular area only/all black
	Dorso-lateral color	DLC	Color of the body on the DL surface	Absent/restricted to scapular area/strongest in scapular area but extends onto entire DL surface/even and covering DL surface
	Lip scale color	LC	Color of the lip scales	Indistinct from head color/demarcated but not distinct from head color/demarcated and white

[6.9–13.9 mya]). Due to our inability to resolve the relationships among *D. nobbi*, *D. australis*, and *D.* sp. nov. by using the mtDNA data set, we estimate divergence between *D. nobbi* and *D.* sp. nov. by using the *RAG1* data set only. The *RAG1* topology suggesting these two species as sister taxa is consistent with the large degree of morphological similarity between the two taxa and is probably a function of saturation of mtDNA signal as opposed to suggesting uncertain relationships among these members of this species group. Using the *RAG1* data, we estimate the divergence between *D. nobbi* and *D.* sp. nov. occurred ~8.61 mya (95% HPD, 3.8–13.1 mya). Divergences within *D. nobbi* firmly place intraspecific diversification within this species in the late Miocene period (3–8 mya), with divergence between the populations of *D.* sp. nov. occurring within the Pio-Pleistocene (2.25 mya; 95% HPD, 0.8–4.1 mya).

Morphological Analyses.—PCA was used initially to reduce the number of morphological and meristic measurements to a fewer number of independent axes. Neither males nor females could be distinguished based on morphometric measurements, with these variables not strongly positively or negatively loaded in PCA results (Table 3). In males, the first two PCs accounted for 64.87% of the observed variation (Table 3). PC2 is negatively loaded for nuchal spine, metacarpal scale, and metatarsal scale counts and moderately positively loaded for right femoral pore and scapular spine counts, attributing to 17.65% of male variation (Table 3). Males with high PC1 scores have higher numbers of femoral and preanal pores, a higher number of spines on the head and scapular regions, irregular scalation between the paravertebral scale rows, a low number of metatarsal scales, and dark throat coloration, accounting for 47.22% of the variation in male characters. Males with high PC2 scores have fewer nuchal spines, metacarpal scales, and metatarsal scales, with a moderate number of right femoral pores and scapular spines, accounting for 17.65% of male variation. Using PC1 scores, *D.* sp. nov. (PC1 = 1.53 ± 0.446; N = 9) exhibits significantly higher PC1 scores (t = −7.12, df = 51, P = 0.000) than *D. nobbi* (PC1 = −0.310 ± 0.755; N = 44). For PC2 scores, *D.* sp. nov. individuals are slightly but significantly higher (t = −2.67, df = 51, P = 0.02; PC2 = 0.685 ± 0.849) than *D. nobbi* (PC2 = −0.017 ± 0.937). Morphological divergences between the two species are further illustrated when PC1 scores are plotted against PC2 scores and the 95% confidence kernel ellipses do not overlap (Fig. 4a).

For females the first two PCs accounted for the majority of morphological variation (59.22%, Table 3). Females with high

Table 2. Average (with SDs) morphometric and meristic character results between *Diporiphora nobbi* and *D.* sp. nov. Refer to Table 1 for a description of characters measured and categories.

| Morphological variable	Male		Female	
	D. nobbi	*D.* sp. nov.	*D. nobbi*	*D.* sp. nov.
SVL	65.93 (±9.16)	62.43 (±6.93)	68.92 (±8.22)	62.34 (±5.81)
AG	29.01 (±4.15)	26.43 (±4.01)	32.23 (±5.23)	28.56 (±3.93)
SL	8.26 (±1.28)	8.19 (±1.15)	8.21 (±1.02)	7.95 (±0.74)
HL	21.25 (±3.40)	20.66 (±2.93)	21.04 (±2.25)	19.77 (±1.49)
HD	10.51 (±1.28)	9.84 (±1.00)	10.33 (±0.94)	9.68 (±0.84)
NW	5.88 (±0.82)	5.83 (±0.81)	5.95 (±0.73)	5.64 (±0.47)
IOW	9.31 (±1.20)	9.36 (±1.14)	9.25 (±0.93)	8.77 (±0.97)
HW	13.92 (±1.76)	13.93 (±1.51)	13.97 (±1.29)	13.40 (±1.09)
ArL	30.13 (±3.87)	29.75 (±2.94)	31.13 (±3.06)	29.74 (±1.86)
LgL	56.08 (±6.87)	54.69 (±5.60)	55.93 (±5.55)	54.10 (±4.43)
McL	6.66 (±0.90)	6.42 (±0.50)	6.66 (±0.85)	6.13 (±0.70)
MtL	13.70 (±1.49)	12.81 (±1.20)	13.34 (±1.48)	12.26 (±1.00)
TaL	166.88 (±31.16)	153.13 (±23.19)	162.03 (±22.45)	137.57 (±15.83)
RFP	1.20 (0–4)	4.56 (4–6)	1.44 (0–3)	3.67 (2–5)
LFP	1.30 (0–3)	4.44 (4–6)	1.46 (0–3)	3.50 (2–4)
RPAP	2.55 (1–3)	4.33 (3–6)	2.73 (0–4)	3.60 (3–4)
LPAP	2.58 (1–4)	4.44 (4–6)	2.63 (0–4)	3.50 (3–4)
McS	17.38 (14–22)	16.56 (16–18)	16.64 (14–20)	16.43 (15–18)
MtS	26.85 (22–32)	24.89 (22–27)	24.93 (21–29)	24.57 (23–26)
ILS	10.33 (9–13)	11.11 (10–13)	10.57 (8–13)	10.43 (8–12)
SLS	10.26 (8–13)	11.33 (11–14)	10.29 (8–12)	10.14 (8–11)
TyW	3.05 (±0.43)	3.34 (±0.38)	3.03 (±0.40)	3.30 (±0.33)
PAS	4.16 (1–8)	5.11 (2–12)	3.74 (1–9)	4.00 (2–6)
UAS	4.95 (1–8)	6.67 (5–8)	5.17 (1–10)	6.43 (6–8)
SUAS	2.47 (0–6)	4.78 (4–6)	2.38 (0–5)	3.71 (2–5)
SS	1.27 (0–6)	3.89 (1–8)	1.67 (0–4)	2.86 (2–4)
NS	3.85 (0–10)	9.11 (5–14)	3.62 (0–9)	8.00 (6–10)
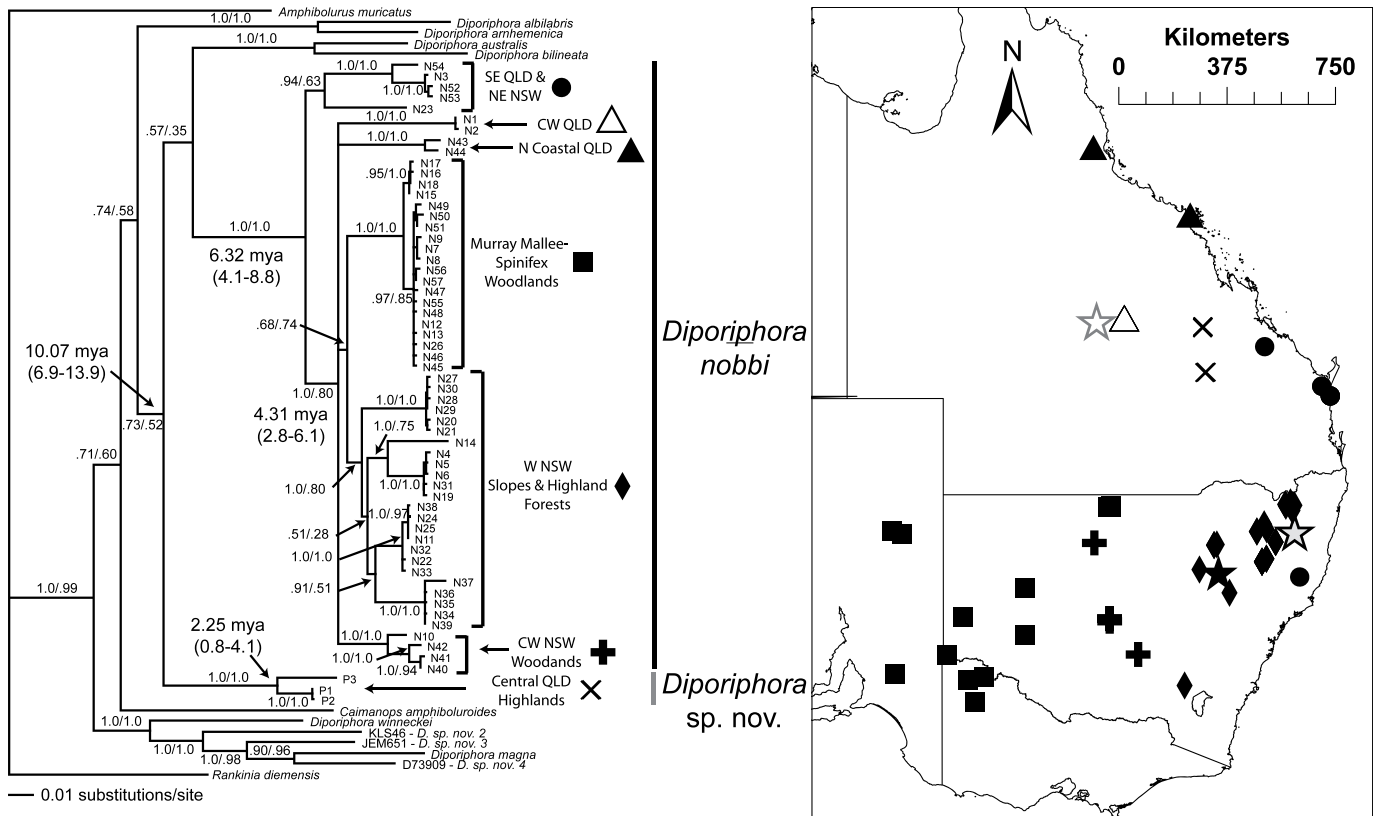
FIG. 2. Bayesian consensus phylogram of mtDNA clades within *Diporiphora nobbi* and a newly identified species (*D.* sp. nov.), including estimated dates for specific nodes and a distribution map of each major clade. Nodal support is shown in the form of Bayesian posterior probabilities from 4 million generations, and estimated nodal dates are median values with 95% confidence intervals displayed in brackets from 10 million generations. Six major mtDNA clades are identified within *D. nobbi*. Clades are generally associated with specific regions, habitat types, or both: SE QLD & NE NSW, solid circle; CW QLD, open triangle; N Coastal QLD, solid triangle; Murray mallee–spinifex Woodlands, solid square; W NSW Slopes and Highlands, solid diamond; and CW NSW Woodlands, plus sign. The distribution of *D.* sp. nov. is shown by the cross sign. The type localities for each of the nominate subspecies within *D. nobbi* are shown (*D. n. nobbi*, open black and gray star; *D. n. coggeri*, solid black star), as is the type locality for the previously synonymized *Wittenagama parnabyi* (open gray and white star).

PC1 scores have high numbers of nuchal, upper auricular and scapular spines, higher femoral pore counts, irregular scalation between enlarged paravertebral rows, and a random or clustered arrangement of nuchal spines separate from PoAF and DLS, accounting for 40.59% of female morphological variation. PC2 accounts for 18.63% of all female morphological variation, indicating individuals with higher numbers of supralabial, metacarpal, and metatarsal scales, higher numbers of upper auricular spines, and fewer scapular spines. Females differ significantly ($t = -5.19$, df = 46, $P = 0.000$) in PC1 between *D.* sp. nov. (1.48 ± 0.484; $N = 7$) and *D. nobbi* ($-0.223 ± 0.84$; $N = 41$) but not PC2 ($t = -0.19$, df = 46, $P = 1.000$; *D.* sp. nov. PC2 = 0.038 ± 0.793; *D. nobbi* PC2 = $-0.039 ± 1.039$). Incomplete morphological divergence is reflected in the confidence ellipse overlap that is seen between *D.* sp. nov. females and *D. nobbi* females when PC scores are plotted against one another in Euclidean space (Fig. 4b).

TAXONOMIC ACCOUNT

Diporiphora phaeospinosa sp. nov.
Figure 5b,d,f,h,j

Holotype.—MVD74128 collected from Bauhinia Station, QLD (25.17°S, 149.20°E).

Paratypes.—Males: QMJ32596, Blackdown Tablelands (23.80°S, 149.13°E); QMJ33335, QMJ33336, QMJ34296, Blackdown Tablelands (23.80°S, 149.07°E); AMR151843, AMR151844, Blackdown Tablelands (23.76°S, 149.10°E); MVD74129 Bauhinia

Station (25.19°S, 149.16°E); QMJ36891, Glenhaughton Station (25.23°S, 148.95°E). Females: QMJ34294, QMJ34295, QMJ36890, Blackdown Tablelands (23.80°S, 149.13°E); QMJ50807, Blackdown Tablelands (23.80°S, 149.10°E); AMR151842, Blackdown Tablelands (23.79°S, 149.09°E); AMR151845, Blackdown Tablelands (23.76°S, 149.10°E); QMJ36892, Reklau Park (23.33°S, 147.50°E); QMJ38591, Glenhaughton Station (25.14°S, 148.57°E). Juveniles: QMJ28495, Blackdown Tableland (23.80°S, 149.13°E); QMJ30267, QMJ38560, QMJ38590, Robinson Gorge (25.28°S, 149.15°E); QMJ38589, Glenhaughton Station (25.23°S, 148.95°E).

Diagnosis and Distinction from Other Species.—*Diporiphora phaeospinosa* is similar in body size and proportion to *D. nobbi*; in fact, the two species cannot be distinguished using any single morphometric trait measured. The main feature distinguishing the two species is the higher number of femoral and preanal pores and nuchal spines in *D. phaeospinosa* in comparison with *D. nobbi*. The PCA (Fig. 4) also identified high numbers of scapular spines, auricular spines, and dark throat coloration in males as significant factors in distinguishing the species. Another distinguishing feature is the presence of enlarged dorso-lateral scales, a feature that is also present in juveniles and adults and that may assist in identifying immature individuals. Both *D. nobbi* and *D. phaeospinosa* lack femoral pores, distinguishing them from their sympatrically distributed sister lineage, the *D. australis/bilineata* species group, which has femoral pores (Witten, 1972).

Description of Holotype.—Adult male SVL, 72.87 mm; AG, 31.85 mm; HL, 25.32 mm; SL, 9.36 mm; HD, 11.32 mm; HW,

FIG. 3. Bayesian consensus phylogram of nuclear DNA (*RAG1* locus) clades within *Diporiphora nobbi* and a newly identified species (*D.* sp. nov.), including estimated dates for specific nodes and a distribution map of each major clade. Nodal support is shown in the form of Bayesian posterior probabilities from 4 million generations, and estimated nodal dates are median values with 95% confidence intervals displayed in brackets from 10 million generations. This analysis confirms the mtDNA result that *D. nobbi* and *D.* sp. nov. are reciprocally monophyletic sister lineages.

15.94 mm; NW, 6.58 mm; IOW, 10.59 mm; ArL, 31.22 mm; McL, 6.59 mm; LgL, 59.79 mm; MtL, 14.08 mm; TaL, 188 mm; RFP, 4; LFP, 4; RPP, 4; LPP, 4; McL, 18; MtL, 26; ILS, 13; SLS, 14, TyW, 3.89 mm; PAS, 8; UAS, 7; SAUS, 5; NS, 9; SS, 4.

Diporiphora phaeospinosa is a robust and large lizard compared with other members of the genus *Diporiphora*. The head is large and angular with a sharp snout that is wider than it is deep. Tympanum has a series of enlarged spine rows extending anteriorly (Fig. 5b). Nuchal spines are separate from the paravertebral scale rows on the dorsum and extend across the base of the head in an uneven manner. Gular folding is absent, and the throat is heavily colored with black extending from the chest across the entire underside of the throat. Infralabial and supralabial scales are clearly demarcated from the darker head coloration and are white.

Scapular folding is strong and arches up across the forearm to contact the paravertebral scale rows. Scapular spines form a row along the scapular fold, but they do not extend along its entire length. Specimen has dark coloration across the entire dorso-lateral surface similar to that observed on the throat. Scattered enlarged scales forming spines are randomly scattered across the entire dorsolateral surface of the body. Specimen has faint darkish colored paravertebral stripes that are not continuous down the extent of the body. Paravertebral scale rows are steeply keeled and distinct from surrounding scales and form uneven rows that are separated by unevenly scattered keeled scales (Fig. 5f). Scales between the paravertebral rows are somewhat reduced toward the distal end of the body and base of the tail. Tail is not compressed, but rounded,

and displays a deep red flush at the base extending the length of the tail in life.

Intraspecific Variation.—Table 2 shows that morphometric characters within *D. phaeospinosa* are directly overlapping with the intraspecific variation observed within *D. nobbi*. Auricular, scapular, and nuchal spine count variation is broader in *D. phaeospinosa* than *D. nobbi*, and although the two species directly overlap *D. phaeospinosa* generally has more spines than *D. nobbi*. Dorsolateral spines and keeling of paravertebral scales are consistently present in *D. phaeospinosa*, with few individuals displaying similar but not identical characters in *D. nobbi*. Analysis of variation in male breeding coloration was not possible from preserved specimens and may provide further distinguishing characteristics between the two species. The breadth of variation possible within *D. phaespinosa* may not be accurately assessed in the current study due to a limited number of specimens available for analysis. In addition, variation as it is currently defined within *D. nobbi* may be altered with further revision of taxonomic relationships among the divergent clades within *D. nobbi*.

Distribution.—The distribution of *D. phaeospinosa* is currently limited to four localities in central western Queensland, representing two discrete regions. The first region is in the Carnarvon Gorge/Bigge Range area, and the second region is in the vicinity of the Blackdown Tablelands. It is currently unknown whether the distribution of the species is continuous, or whether these discrete regions represent disjunct populations, because the number of specimens known for this new species are currently limited. Our genetic data suggest that the two

TABLE 3. Summary of principal component (PC) loadings across morphological variables for both male and female *Diporiphora nobbi* and *D.* sp. nov. analyses, respectively. Values in bold indicate measurements that are considered important (PC loading < 0.5).

Variable	Male PC1	Male PC2	Female PC1	Female PC2
NS	**3.749**	**−1.241**	**2.9**	0.345
RFP	**1.131**	**0.533**	**0.854**	−0.238
LFP	**1.011**	0.301	**0.704**	−0.238
RPAP	**0.592**	0.192	0.302	−0.332
LPAP	**0.647**	0.275	0.393	−0.199
MCS	−0.179	**−1.08**	−0.13	**1.179**
MTS	**−0.691**	**−2.083**	−0.311	**1.632**
ILS	0.452	−0.163	—	—
SLS	0.381	−0.202	0.021	**0.543**
PAS	**0.762**	0.373	0.483	−0.264
UAS	**0.86**	0.073	**0.689**	**0.742**
SUAS	**0.855**	0.231	—	—
SS	**0.771**	**0.806**	**0.515**	**−0.544**
NSP	**1.002**	0.255	**0.987**	0.07
PVS	—	—	0.171	0.065
RPVS	—	—	0.182	0.023
SBWPVS	**0.589**	0.297	**0.569**	0.018
TC	**1.148**	0.327	—	—
Eigenvalue	23.3	8.71	12.33	5.66
% variance explained	47.22	17.65	40.59	18.63

regions occupied by the species are genetically distinct; however, this may simply be a function of isolation by distance rather than suggestive of discrete genetic populations due to limited sampling in intermittent areas. Genetic and morphological analyses suggest that *D. phaeospinosa* is allopatric with respect to the distribution of its congener *D. nobbi*. Further analysis of the species distribution would be required to resolve these issues.

Etymology.—The specific epithet *phaeospinosa* is a composite from the Latin root terms *phaeo* (dark) and *spinos* (spiny) describing the main distinguishing morphological features of this species.

DISCUSSION

Using an analysis of morphology and genetics, we show extensive diversity within *D. nobbi* and uncover a previously undescribed species within this species group, *D. phaeospinosa*. This new species is highly divergent from nominal *D. nobbi* individuals by using both molecular (Figs. 2, 3) and morphological characters (Fig. 4). We also describe high levels of genetic diversity within nominal *D. nobbi* associated with distinct geographic regions and habitat types across the broad distribution of this species. Here, we describe the ramifications of our work on perceived species boundaries within the *D. nobbi* species complex, and we discuss possible hypotheses to explain the potential diversification mechanisms within the *D. nobbi* species complex and the biogeographic diversity within nominal *D. nobbi*.

Species Boundaries and Taxonomy within the D. nobbi Species Group.—Our analysis of molecular and morphological variation within *D. nobbi* shows no support for current subspecies delineations, *D. n. nobbi* and *D. n. coggeri*, within the *D. nobbi* complex. Both holotypes for these subspecies seem to occur within the geographic region encompassed by the western NSW slopes and highland forests mtDNA subclade (Fig. 2) and also cannot be resolved as subspecies using the *RAG1* dataset (Fig. 3). Similarly, there is no support for the previously described *W. parnabyi* (Wells and Wellington, 1985), later synonymized within *D. nobbi* (Shea and Sadlier, 1999), as distinct from *D. nobbi*. This holotype is probably associated with the mtDNA subclade from central western QLD. Our
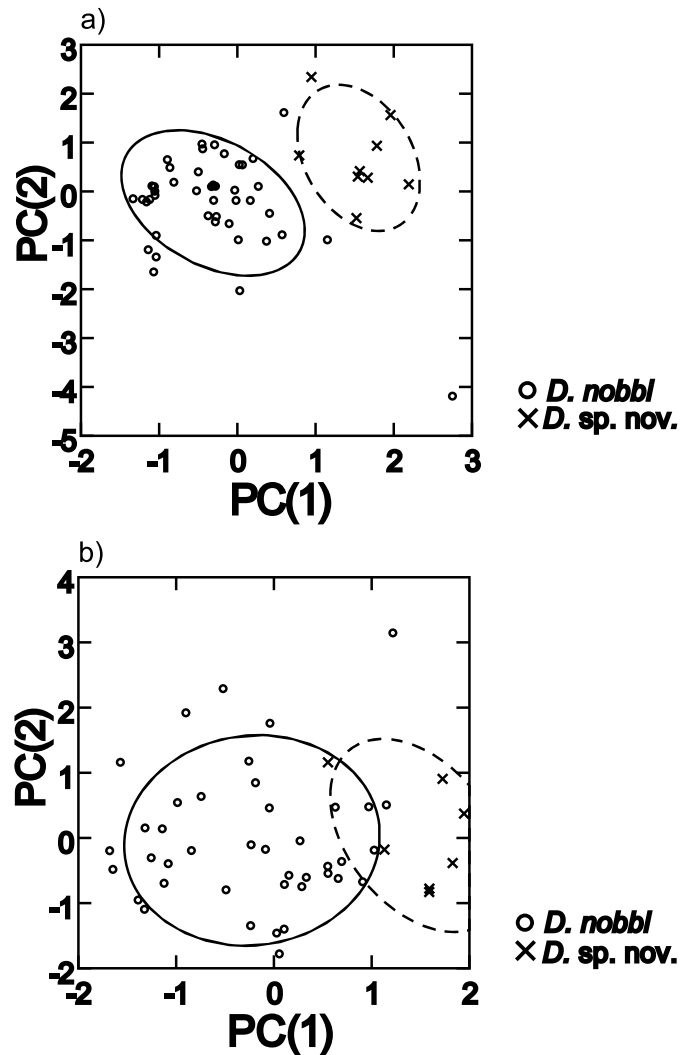

FIG. 4. Principal components analysis of male (a) and female (b) morphological data based on genetic species described in the genetic analyses. Principal components (PCs) are calculated from a covariance matrix on an optimal set of morphological characters. PC1 is plotted against PC2 in Euclidian space. PC1 explains 47.22 and 40.59% of the variation and values are significantly different between *D. nobbi* and *D.* sp. nov. in the male and female data, respectively. PC2 explains 17.65 and 18.63% of the variation in the male and female data, respectively. PC2 is only significantly different between *D. nobbi* and *D.* sp. nov. for the male data. Refer to Table 3 for an explanation of the variable loadings for PC1 and PC2 for both the male and female data.

results show that there is considerable diversity within nominate *D. nobbi*. However, with the current data, an analysis of morphological boundaries within the *D. nobbi* lineage and among molecular subclades was not possible due to low number of specimens with material available for both molecular and morphological analyses.

Even with an analysis of morphological diversity within nominate *D. nobbi*, it is unlikely that the currently described subspecies, *D. n. nobbi* and *D. n. coggeri* (Witten, 1972) would be resolved as morphologically distinct species or in fact distinct subspecies, and we recommend that the two subspecies be synonymized under the name of *D. nobbi*. Alternatively, differences between these two groups may be a function of genetic subdivision within this region observed within our own mtDNA data (Fig. 2) and also observed within many other species throughout the western NSW slopes region (Chapple et al., 2005; O'Meally and Colgan, 2005; Colgan et al., 2009). Given the high levels of molecular diversity within nominate *D. nobbi*,
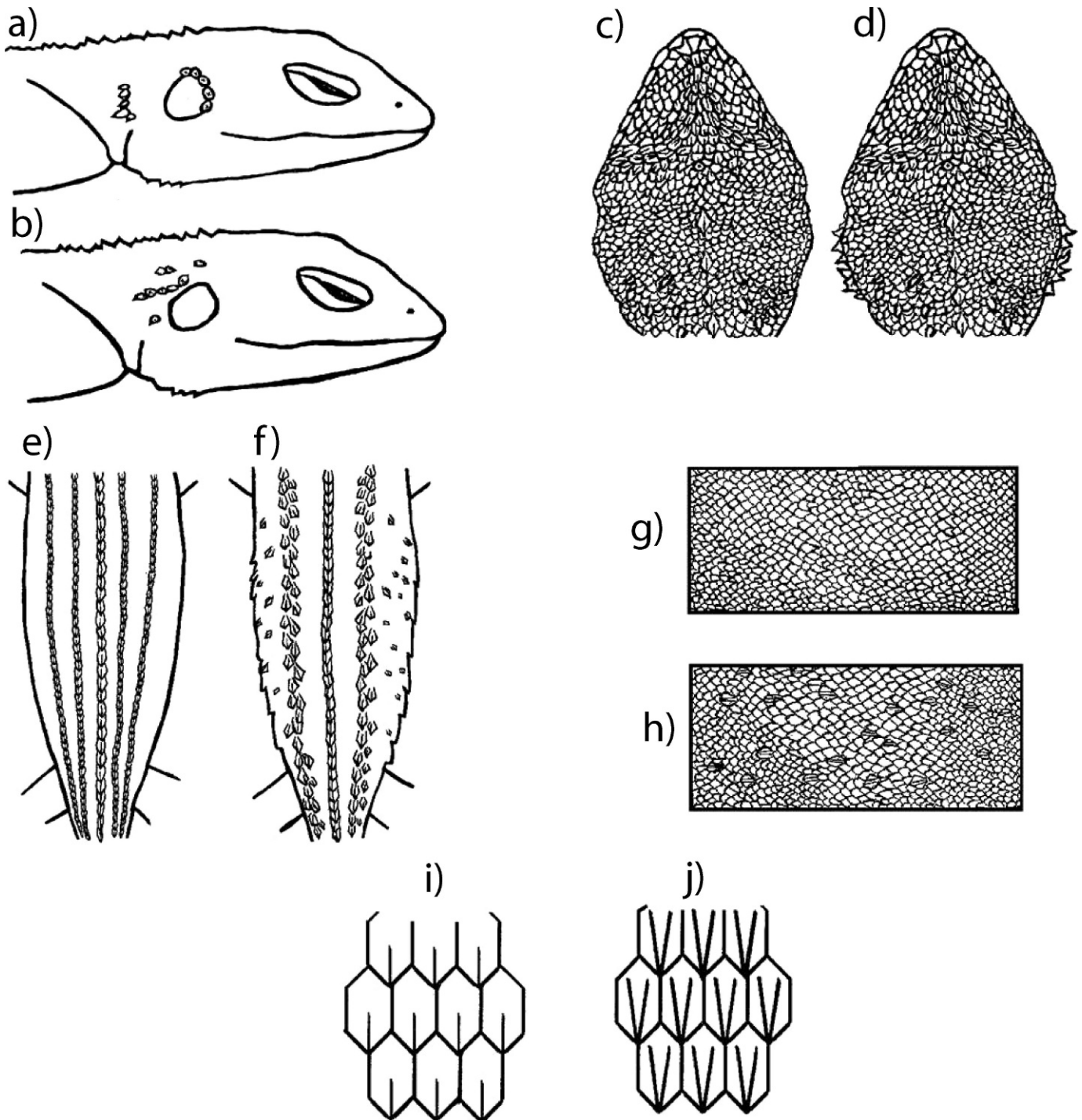
FIG. 5. Diagnostic drawings of morphological features distinguishing between *Diporiphora nobbi* (a, c, e, g, i) and *Diporiphora phaeospinosa* (b, d, f, h, j). Illustrations show the arrangement of postauricular spines, lateral view, stylized (a–b); upper auricular spines and nuchal spine arrangement, dorsal view, detailed (c–d), paravertebral and dorso-lateral scale keeling and regularity, dorsal view, stylized (e–f); dorso-lateral scale keeling, lateral view, detailed (g–h); and differences between strength of scale keeling, close-up (i–j). Illustrations by Corrine Edwards.

it is possible that future molecular and morphological analyses could find support for raising *D. parnabyi* and several other subclades within nominate *D. nobbi* to species status. However, there is no support warranting the use of a distinct genus name, as ascribed by Wells and Wellington (1985).

Diversification and Biogeography of the D. nobbi Species Complex.—Our divergence analyses suggest that the split between *D. nobbi* and *D. phaeospinosa* occurred between 4 and 14 mya, with splits between the *D. nobbi* lineage and the *D.*

australis/bilineata lineage occurring at a similar time (between 8 and 19 mya). Due to the similar timing of these events, it is likely that the developing aridity in Australia during the mid-late Miocene, leading to dramatic changes in forest types (Bowler, 1976; Macphail, 1997; Kershaw et al., 2003), is associated with diversification of the eastern Australian *Diporiphora australis-nobbi* lineage. Previous analysis has suggested a northern origin for the *D. australis* lineage (Edwards and Melville, 2010), which has only recently been present in

southern QLD and northern NSW as of the mid-late Pleistocene (Hocknull et al., 2007). Given the much deeper age of nodes within the *D. nobbi* species complex (Figs. 2, 3) this lineage probably occupied a more southerly distribution historically, and these two sister lineages have only recently been almost entirely sympatrically distributed.

Both *D. australis* and *D. nobbi* currently occupy dry woodland habitats, habitats that rapidly expanded during the mid-late Miocene climate shift (Bowler, 1976; Macphail, 1997; Kershaw et al., 2003). *Diporiphora phaeospinosa*, in contrast, seems to be restricted to the wetter eucalypt forests in central southern QLD, a region harboring many endemic and relictual species of snail (A. F. Hugall, pers. comm.). Diversification within the *D. nobbi* species complex is probably a result of sweeping climatic and environmental change across the Australian continent at this time (Bowler, 1976; Macphail, 1997; Kershaw et al., 2003) that either led to vicariance between the *D. nobbi* and *D. phaeospinosa* populations or to adaptive evolution within *D. nobbi* to favor the broadly distributed dry woodland habitats coincident with expansion into these newly available habitats. Many groups of Australian lizards have shown rapid adaptive radiations during the mid-late Miocene period, including other members of the subfamily Amphibolurinae (e.g., *Ctenophorus*, Melville et al., 2001), Elapidae (Sanders et al., 2008), and much more diverse genera, such as *Lerista* (Skinner and Lee, 2009) and *Ctenotus* (Rabosky et al., 2007).

Unlike *D. australis* (Edwards and Melville, 2010) and some other northern QLD woodland taxa, the distribution of genetic variation within *D. nobbi* cannot be predicted by known biogeographic barriers. This is consistent with the hypothesis that biogeographic patterns in woodland taxa may be harder to predict than those of rainforest taxa (James and Moritz, 2000). Rather, our mtDNA genetic data suggest that diversity within *D. nobbi* is associated with specific habitat types. mtDNA clades within *D. nobbi* are specifically associated with the northern QLD Tablelands forests, central western QLD woodlands, coastal forests and swamps of southeastern QLD and northeastern NSW, western slopes and highland forests of NSW, central NSW woodlands and the Murray River basin mallee–spinifex woodlands of western NSW, eastern South Australia (SA), and northwestern Victoria (VIC). Whereas our current nuclear data do not show a similar pattern, the marker used here is not particularly appropriate for testing population level associations. Our results provide preliminary evidence that mtDNA divergence among *D. nobbi* subclades may be associated with ecological differentiation, a response common in many of the adaptive radiations reported from rapidly evolving arid regions in Australia (Melville et al., 2001, 2006; Byrne et al., 2008). However, to test this hypothesis increased genetic and morphological sampling in conjunction with ecological information is required from across the distribution of the species.

Previous population genetic studies using both mtDNA and allozyme markers have shown deeply divergent breaks among *D. nobbi* populations in one region of NSW, which was also identified in the current study. Driscoll and Hardy (2005) alluded to a distinction between *D. nobbi* populations occupying a fragmented agricultural landscape versus continuous mallee–spinifex woodlands in southern central NSW and separated by the Lachlan River, in a region associated with meeting range limits of many sister taxa without any obvious steep ecological gradient. The two divergent populations were not exchanging genes, and both were occupying mallee woodlands with a spinifex understorey. Driscoll and Hardy (2005) probably identified the junction between what we have termed the central western NSW woodland clade and the mallee–spinifex clade; however, both are occupying the same mallee–spinifex habitat. Driscoll and Hardy (2005) also uncovered weak evidence for increased dispersal within the agricultural landscape. It is possible that western woodland

populations may have been able to move into the mallee habitat postdisturbance and local extinction of the woodland clade; alternatively, the Lachlan River may be providing the divergence mechanism between these two clades as opposed to simply habitat differentiation.

Our study also identifies high levels of differentiation among *D. nobbi* populations across QLD and NSW, with mtDNA subclades associated with coastal forests and swamps of southeastern QLD/northeastern NSW, northern QLD wet/dry tropical areas, central QLD woodlands, and the western slopes of NSW. Divergence among the former two subclades could be associated with the St. Lawrence Gap, seen in other woodland (James and Moritz, 2000; Edwards and Melville, 2010) and rain forest taxa (Stuart-Fox et al., 2001; Moussalli et al., 2005; Joseph and Omland, 2009). However, divergences across this barrier are generally considered to correspond to the Pleistocene (James and Moritz, 2000; Stuart-Fox et al., 2001; Moussalli et al., 2005; Joseph and Omland, 2009; Edwards and Melville, 2010). Alternatively, divergence among these QLD and NSW subclades could have arisen through differentiation across steep environmental and habitat gradients.

A combination of morphological and molecular information is not only invaluable in the description of cryptic diversity but also provides insight into the evolutionary processes driving diversification within closely related species. Alpha and higher level taxonomy in morphologically homoplasic groups, e.g., Amphibolurinae, require such information for accurate taxonomic revision. The taxonomic history of the *D. nobbi* species complex and cryptic diversity habored within it is indicative of this problem in amphibolurine alpha taxonomy. Although our study identifies some potential hypotheses explaining diversification within the *D. nobbi* species complex and population differentiation within *D. nobbi*, this study is by no means a complete treatment of diversity within this lineage. Much more information is required to definitively test diversification hypotheses within *D. nobbi*. This is true for eastern Australian woodland environments in general that contain many widely distributed species but that may, in fact, be species complexes, crossing steep environmental gradients.

LITERATURE CITED

BOWLER, J. M. 1976. Aridity in Australia: age, origins and expression in aeolian landforms and sediments. Earth Science Reviews 12:279–310.

BYRNE, M., D. K. YEATES, L. JOSEPH, M. KEARNEY, J. BOWLER, M. A. J. WILLIAMS, S. COOPER, S. C. DONNELLAN, J. S. KEOGH, R. LEYS, J. MELVILLE, D. J. MURPHY, N. PORCH, AND K. H. WYRWOLL. 2008. Birth of a biome: insights into the assembly and maintenance of the Australian arid zone biota. Molecular Ecology 17:4398–4417.

CHAPPLE, D. G., J. S. KEOGH, AND M. N. HUTCHINSON. 2005. Substantial genetic substructuring in southeastern and alpine Australia

revealed by molecular phylogeography of the *Egernia whitii* (Lacertilia: Scincidae) species group. Molecular Ecology 14:1279–1292.

Cogger, H. G. 2000. Reptiles and Amphibians of Australia. Reed New Holland, Sydney, Australia.

Colgan, D. J., D. O'Meally, and R. A. Sadlier. 2009. Phylogeographic patterns in reptiles on the New England Tablelands at the south-western boundary of the McPherson-Macleay overlap. Australian Journal of Zoology 57:317–328.

Covacevich, J., P. Couper, R. E. Molnar, G. Witten, and W. Young. 1990. Miocene dragons from Riversleigh: new data on the history of the family Agamidae (Reptilia: Squamata) in Australia. Memoirs of the Queensland Museum 29:339–360.

Dolman, G., and C. Moritz. 2006. A multilocus perspective on refugial isolation and divergence in rainforest skinks (*Carlia*). Evolution 60:573–582.

Driscoll, D. A., and C. M. Hardy. 2005. Dispersal and phylogeography of the agamid lizard *Amphibolurus nobbi* in fragmented and continuous habitat. Molecular Ecology 14:1613–1629.

Drummond, A., and A. Rambaut. 2007. BEAST: Bayesian evolutionary analysis by sampling trees. BMC Evolutionary Biology 7:214.

Drummond, A. J., S. Y. W. Ho, M. J. Phillips, and A. Rambaut. 2006. Relaxed phylogenetics and dating with confidence. PLoS Biology 4:699–710.

Edwards, D. L., and J. Melville. 2010. Phylogeographic analysis detects congruent biogeographic patterns between a woodland agamid and Australian wet tropics taxa despite disparate evolutionary trajectories. Journal of Biogeography 37:1543–1556.

Evans, S. E., G. V. R. Prasad, and B. K. Manhas. 2002. Fossil lizards from the Jurassic Kota formation of India. Journal of Vertebrate Paleontology 22:229–312.

Greer, A. E. 1989. The Biology and Evolution of Australian Lizards. Surrey Beatty and Sons, Chipping Norton, NSW, Australia.

Hocknull, S. A., J. X. Zhao, Y. X. Feng, and G. E. Webb. 2007. Responses of Quaternary rainforest vertebrates to climate change in Australia. Earth and Planetary Science Letters 264:317–331.

Hugall, A. F., and M. S. Y. Lee. 2004. Molecular claims of Gondwanan age for Australian agamid lizards are untenable. Molecular Biology and Evolution 21:2102–2110.

Hugall, A. F., R. Foster, and M. S. Y. Lee. 2007. Calibration choice, rate smoothing and the pattern of tetrapod diversification according to the long nuclear gene *RAG1*. Systematic Biology 56:543–563.

Hugall, A. F., R. Foster, M. Hutchinson, and M. S. Y. Lee. 2008. Phylogeny of Australasian agamid lizards based on nuclear and mitochondrial genes: implications for morphological evolution and biogeography. Biological Journal of the Linnean Society 93:343–358.

James, C. H., and C. Moritz. 2000. Intraspecific phylogeography in the sedge frog *Litoria fallax* (Hylidae) indicates pre-Pleistocene vicariance of an open forest species from eastern Australia. Molecular Ecology 9:349–358.

Joseph, L., and K. E. Omland. 2009. Phylogeography: its development and impact in Australo-Papuan ornithology with special reference to paraphyly in Australian birds. Emu 109:1–23.

Kershaw, P., P. Moss, and S. van der Kaars. 2003. Causes and consequences of long-term climatic variability on the Australian continent. Freshwater Biology 48:1274–1283.

Macey, J. R., A. Larson, N. B. Ananjeva, Z. Fang, and T. J. Papenfuss. 1997. Two novel gene orders and the role of light-strand replication in rearrangement of the vertebrate mitochondrial genome. Molecular Biology and Evolution 14:91–104.

Macey, J. R., J. A. Schulte, A. Larson, N. B. Ananjeva, Y. Z. Wang, R. Pethiyagoda, N. Rastegar-Pouyani, and T. J. Papenfuss. 2000. Evaluating trans-tethys migration: an example using acrodont lizard phylogenetics. Systematic Biology 49:233–256.

Macphail, M. K. 1997. Late Neogene climates in Australia: fossil pollen- and spore-based estimates in retrospect and prospect. Australian Journal of Botany 45:425–464.

Melville, J., J. A. Schulte II, and A. Larson. 2001. A molecular phylogenetic study of ecological diversification in the Australian lizard genus *Ctenophorus*. Journal of Experimental Zoology (Molecular Development and Evolution) 291:339–353.

Melville, J., L. J. Harmon, and J. B. Losos. 2006. Intercontinental community convergence of ecology and morphology in desert lizards. Proceedings of the Royal Society of London Series B Biological Sciences 273:557–563.

Melville, J., L. P. Shoo, and P. Doughty. 2008. Phylogenetic relationships of the heath dragons (*Rankinia adelaidensis* and *R. parviceps*) from the south-western Australian biodiversity hotspot. Australian Journal of Zoology 56:159–171.

Melville, J., J. Hale, G. Mantziou, N. B. Ananjeva, K. Milto, and N. Clemann. 2009. Historical biogeography, phylogenetic relationships and intraspecific diversity of agamid lizards in the central Asian deserts of Kazakhstan and Uzbekistan. Molecular Phylogenetics and Evolution 53:99–112.

Moritz, C., J. L. Patton, C. J. Schneider, and T. B. Smith. 2000. Diversification of rainforest faunas: an integrated molecular approach. Annual Review of Ecology and Systematics 31:533–563.

Moussalli, A., A. F. Hugall, and C. Moritz. 2005. A mitochondrial phylogeny of the rainforest skink genus *Saproscincus*, Wells and Wellington (1984). Molecular Phylogenetics and Evolution 34:190–202.

Moussalli, A., C. Moritz, S. E. Williams, and A. C. Carnaval. 2009. Variable responses of skinks to a common history of rainforest fluctuation: concordance between phylogeography and palaeo-distribution models. Molecular Ecology 18:483–499.

O'Meally, D., and D. Colgan. 2005. Genetic ranking for biological conservation using information from multiple species. Biological Conservation 122:395–407.

Posada, D., and K. A. Crandall. 1998. Modeltest: testing the model of DNA substitution. Bioinformatics 14:817–818.

Rieppel, O., A. Walker, and I. Odhiambo. 1992. A preliminary report on a fossil chamaeleonine (Reptilia: Chamaeleoninae) skull from the Miocene of Kenya. Journal of Herpetology 26:77–80.

Robinson, M. D., and T. R. Van Devender. 1973. Miocene lizards from Wyoming and Nebraska. Copeia 1973:698–704.

Rabosky, D. L., S. C. Donnellan, A. L. Talaba, and I. J. Lovette. 2007. Exceptional among-lineage variation in diversification rates during the radiation of Australia's most diverse vertebrate clade. Proceedings of the Royal Society B Biological Sciences 274:2915–2923.

Rambaut, A., and A. J. Drummond. Tracer V1.6 [Internet]. 2005 [cited 2011 Oct 5]. Available from: http://tree.bio.ed.ac.uk/software/tracer/.

Ronquist, F., and J. P. Huelsenbeck. 2003. MrBayes 3: Bayesian phylogenetic inference under mixed models. Bioinformatics 19:1572–1574.

Sanders, K. L., M. S. Y. Lee, R. Leys, R. Foster, and J. S. Keogh. 2008. Molecular phylogeny and divergence dates for Australasian elapids and sea snakes (Hydrophiinae): evidence from seven genes for rapid evolutionary radiations. Journal of Evolutionary Biology 21:682–695.

Schneider, C. J., M. Cunningham, and C. Moritz. 1998. Comparative phylogeography and the history of endemic vertebrates in the wet tropics rainforests of Australia. Molecular Ecology 7:487–498.

Schulte, J. A., J. Melville, and A. Larson. 2003. Molecular phylogenetic evidence for ancient divergence of lizard taxa either side of Wallace's Line. Proceedings of the Royal Society of London Series B Biological Sciences 270:597–603.

Shea, G. M., and R. A. Sadlier. 1999. A catalogue of the non-fossil amphibian and reptile type specimens in the collection of the Australian Museum: types currently, previously and purportedly present. Technical Report of the Australian Museum 15:1–91.

Shoo, L. P., R. Rose, P. Doughty, J. J. Austin, and J. Melville. 2008. Diversification patterns of pebble-mimic dragons are consistent with historical disruption of important habitat corridors in arid Australia. Molecular Phylogenetics and Evolution 48:528–542.

Skinner, A., and M. S. Y. Lee. 2009. Body-form evolution in the scincid lizard clade *Lerista* and the mode of macroevolutionary transitions. Evolutionary Biology 36:292–300.

Smith, K. L., L. J. Harmon, L. P. Shoo, and J. Melville. 2011. Evidence of constrained phenotypic evolution in a cryptic species complex of agamid lizards. Evolution 65:976–992.

Stamatakis, A., P. Hoover, and J. Rougemont. 2008. A rapid bootstrap algorithm for the RAxML web-servers. Systematic Biology 75:758–771.

Stuart-Fox, D. M., C. J. Schneider, C. Moritz, and P. J. Couper. 2001. Comparative phylogeography of three rainforest-restricted lizards from mid-east Queensland. Australian Journal of Zoology 49:119–127.

Thompson, J. D., T. J. Gibson, F. Plewniak, F. Jeanmougin, and D. G. Higgins. 1997. The ClustalX windows interface: flexible strategies for multiple sequence alignment aided by quality analysis tools. Nucleic Acids Research 24:4876–4882.

WELLS, R. W., AND C. R. WELLINGTON. 1985. A classification of the
    Amphibia and Reptilia of Australia. Australian Journal of Herpe-
    tology Supplementary Series 1:1–61.
WITTEN, G. J. 1972. A new species of *Amphibolurus* from eastern
    Australia. Herpetologica 28:191–195.

ZEROVA, G. A., AND V. R. CHKHIKVADZE. 1984. The review of Cenozoic
    lizards and snakes in USSR. News Georgian SSR Academy of
    Sciences. Series: Biology 10:319–325. [In Russian.]

APPENDIX 1. Genetic samples used in molecular analyses. Haplotype numbers, GenBank numbers, registration details, and site details are outlined for each sample. Samples also used in morphological analyses are specified.

Lab no.	Haplotype	ND2 GenBank	RAG1 GenBank	Morphology[a]	Sex[b]	Site[c]	Registration no.	Tissue no.	Museum	Latitude	Longitude
DLE129	N1	JN627101	—	N	—	25 km N Alpha	—	Z10040	Mus. VIC	−23.4822	146.6480
DLE135	N2	JN627050	—	Y	F	25 km N Alpha	D74123	Z10044	Mus. VIC	−23.4822	146.6480
DLE136	N1	JN627052	JN627123	Y	M	25 km N Alpha	D74124	Z10045	Mus. VIC	−23.4822	146.6480
DLE137	N1	JN627085	JN627113	Y	M	25 km N Alpha	D74125	Z10046	Mus. VIC	−23.4807	146.6452
DLE140	P1	JN627087	—	Y	M	Bauhinia Stn.	D74128	Z10049	Mus. VIC	−25.1743	149.2046
DLE141	P2	JN627088	JN627115	Y	M	Bauhinia Stn.	D74129	Z10050	Mus. VIC	−25.1865	149.1618
DLE145	N3	JN627110	JN627117	Y	M	Maryborough	D74132	Z10054	Mus. VIC	−25.6046	152.8121
DLE146	N3	JN627111	JN627125	Y	M	Maryborough	D74133	Z10055	Mus. VIC	−25.6046	152.8121
DLE154	N4	JN627105	JN627127	N	—	Pilliga Forest, Narribri	—	Z10063	Mus. VIC	−30.5657	149.4522
DLE161	N5	JN627086	JN627128	Y	M	Pilliga Forest, Narribri	D74139	Z10070	Mus. VIC	−30.5457	149.5389
DLE162	N6	JN627089	—	Y	M	Pilliga Forest, Narribri	D74140	Z10071	Mus. VIC	−30.5667	149.4513
DLE164	N7	JN627094	—	N	—	140 km N Ivanhoe	—	Z10073	Mus. VIC	−31.8998	143.5610
DLE167	N8	JN627045	—	N	—	Gol Gol	—	Z10185	Mus. VIC	−33.3795	143.5503
DLE168	N7	JN627053	—	Y	M	140 km N Ivanhoe	D74141	Z10186	Mus. VIC	−31.8953	143.5599
DLE169	N9	JN627062	—	Y	M	140 km N Ivanhoe	D74142	Z10187	Mus. VIC	−31.8999	143.5607
DLE170	N8	JN627091	—	Y	M	Gol Gol	D74143	Z10188	Mus. VIC	−33.3796	143.5502
DLE171	N8	JN627063	JN627119	Y	F	Gol Gol	D74144	Z10189	Mus. VIC	−33.3796	143.5502
DLE172	N10	JN635331	JN627124	Y	F	West Wyalong	D74145	Z10190	Mus. VIC	−33.9821	147.0816
DLE173	N10	JN627108	—	Y	F	West Wyalong	D74146	Z10191	Mus. VIC	−33.9823	147.0833
DLE174	N11	JN627081	—	Y	F	Bolivia Hill	R 134983	269	Aust. Mus.	−29.4833	151.9000
DLE175	N12	JN627028	—	Y	M	19.7 km N Coombah RdHs	R 130998	338	Aust. Mus.	−32.8167	141.6167
DLE176	N13	JN627054	—	Y	F	19.7 km N Coombah RdHs	R 130999	339	Aust. Mus.	−32.8167	141.6167
DLE177	N14	JN627093	JN627121	N	J	35 km W Yass	R 135336	548	Aust. Mus.	−34.9500	148.5333
DLE178	N15	JN627046	JN627120	Y	F	90 km NE Bourke	R 141023	1283	Aust. Mus.	−29.3714	146.2333
DLE179	N16	JN627064	—	N	J	90 km NE Bourke	R 141024	1284	Aust. Mus.	−29.3431	146.2314
DLE180	N17	JN627065	—	Y	M	90 km NE Bourke	R 141025	1285	Aust. Mus.	−29.3611	146.2242
DLE181	N18	JN627034	—	N	J	90 km NE Bourke	R 141026	1286	Aust. Mus.	−29.3833	146.1500
DLE182	P3	JN627029	JN627116	Y	F	Blackdown Tbld.	R 151842	5009	Aust. Mus.	−23.7911	149.0939
DLE183	P3	JN627041	—	Y	M	Blackdown Tbld.	R 151843	5010	Aust. Mus.	−23.7586	149.1025
DLE184	P3	JN627038	JN627114	Y	M	Blackdown Tbld.	R 151844	5011	Aust. Mus.	−23.7586	149.1025
DLE185	P3	JN627030	JN627133	Y	F	Blackdown Tbld.	R 151845	5012	Aust. Mus.	−23.7586	149.1025
DLE186	N19	JN627109	—	Y	M	Cassilis-Coolah Rd.	R 152062	5301	Aust. Mus.	−32.0550	149.9333
DLE187	N20	JN627035	—	Y	M	Moonbi Ranges	R 152046	5338	Aust. Mus.	−30.9925	151.0833
DLE188	N21	JN627066	—	N	J	Moonbi Ranges	R 152079	5340	Aust. Mus.	−30.9925	151.0833
DLE189	N21	JN627033	—	N	J	Moonbi Ranges	R 152080	5342	Aust. Mus.	−30.9925	151.0833
DLE190	N22	JN627067	JN627134	Y	M	Torrington SF	R 152098	5459	Aust. Mus.	−29.3392	151.6914
DLE191	N23	JN627082	JN627112	N	J	Boonoo Boonoo NP	R 152341	6129	Aust. Mus.	−31.5564	152.1269
DLE193	N24	JN627047	JN627135	N	J	Pyes Creek Rd.	R 159836	6488	Aust. Mus.	−29.2353	151.8372
DLE194	N25	JN635332	—	N	J	Bolivia Hill	R 159768	6555	Aust. Mus.	−29.3214	151.9181
DLE196	N26	JN627068	—	Y	M	Warrakoo Stn.	R 153217	7113	Aust. Mus.	−33.9858	141.1181
DLE197	N27	JN627095	JN627130	Y	F	2 km N Tamworth	R 157284	7232	Aust. Mus.	−31.0850	150.9472
DLE198	N28	JN627042	—	Y	F	2 km N Tamworth	R 157285	7233	Aust. Mus.	−31.0850	150.9472
DLE199	N29	JN627037	—	Y	F	2 km N Tamworth	R 157286	7234	Aust. Mus.	−31.0850	150.9472
DLE200	N20	JN627097	—	Y	F	2 km N Tamworth	R 157287	7235	Aust. Mus.	−31.0850	150.9472
DLE201	N30	JN627036	—	Y	F	2 km N Tamworth	R 157288	7236	Aust. Mus.	−31.0850	150.9472
DLE202	N31	JN627106	—	Y	M	Warrumbungle NP	R 156048	7613	Aust. Mus.	−31.3289	148.9967
DLE203	N32	JN627055	—	N	J	Torrington SF	R 157100	7933	Aust. Mus.	−29.2944	151.6772
DLE204	N33	JN627056	—	Y	M	Torrington SF	R 157201	8121	Aust. Mus.	−29.2944	151.6772
DLE205	N34	JN627102	—	Y	M	Yarrowick	R 157018	8150	Aust. Mus.	−30.4725	151.3714
DLE206	N35	JN627031	—	Y	M	Yarrowick	R 157023	8154	Aust. Mus.	−30.4725	151.3714
DLE207	N35	JN627103	—	Y	M	Yarrowick	R 157024	8156	Aust. Mus.	−30.4725	151.3714
DLE208	N36	JN627032	—	Y	F	Bundarra-Inverell Rd.	R 157074	8161	Aust. Mus.	−30.0747	151.0967
DLE209	N37	JN627099	JN627131	Y	M	Barraba Rd.	R 157216	8162	Aust. Mus.	−30.1422	150.7872
DLE210	N37	JN627069	JN627129	Y	M	Barraba Rd.	R 157217	8164	Aust. Mus.	−30.1450	150.7869
DLE211	N24	JN627048	—	N	J	Bolivia Hill	R 157221	8170	Aust. Mus.	−29.3372	151.8944
DLE212	N38	JN627070	—	N	J	Bolivia Hill	R 157232	8192	Aust. Mus.	−29.3264	151.9631
DLE213	N39	JN627027	—	Y	M	Copeton	R 157218	8307	Aust. Mus.	−29.9167	151.0167
DLE214	N40	JN627071	—	N	—	35 km from Mt Hope	R 156632	8732	Aust. Mus.	−32.9467	146.1922
DLE215	N41	JN627025	—	Y	F	35 km from Mt Hope	R 156683	8777	Aust. Mus.	−32.8622	146.1894
DLE216	N41	JN627057	JN627132	Y	F	35 km from Mt Hope	R 156684	8778	Aust. Mus.	−32.8622	146.1894
DLE217	N41	JN627058	—	Y	M	35 km from Mt Hope	R 156685	8779	Aust. Mus.	−32.8622	146.1894

APPENDIX 1. Continued.

Lab no.	Haplotype	ND2 GenBank	RAG1 GenBank	Morphology[a]	Sex[b]	Site[c]	Registration no.	Tissue no.	Museum	Latitude	Longitude
DLE218	N40	JN627051	—	Y	F	35 km from Mt Hope	R 156686	8780	Aust. Mus.	−32.8622	146.1894
DLE231	N42	JN627107	—	N	J	Gundabooka NP	R 164801	—	Aust. Mus.	−30.5000	145.7167
DLE232	N43	JN627083	JN627122	Y	M	Airlie Beach	R 164849	—	Aust. Mus.	−20.2667	148.7000
DLE242	N44	JN627092	—	Y	F	Kirrama	J82745	—	QLD Mus.	−18.1536	145.6833
JEM196	N12	JN627104	—	Y	F	Wyperfeld NP	D71317	Z10192	Mus. VIC	−35.4594	142.0069
JEM197	N45	JN627078	—	N	—	Wyperfeld NP	D71318	Z10193	Mus. VIC	−35.4594	142.0069
JEM198	N12	JN627084	—	N	—	Wyperfeld NP	D71319	Z10194	Mus. VIC	−35.4594	142.0069
JEM199	N46	JN627079	—	N	—	Wyperfeld NP	D71320	Z10195	Mus. VIC	−35.4594	142.0069
JEM200	N12	JN627061	—	N	—	Wyperfeld NP	D71321	Z7876	Mus. VIC	−35.4594	142.0069
JEM222	N47	JN627090	—	N	—	Murray-Sunset NP	D71343	Z7875	Mus. VIC	−34.7597	141.7758
JEM223	N12	JN627075	—	N	—	Murray-Sunset NP	D71344	Z7874	Mus. VIC	−34.7597	141.7758
JEM224	N12	JN627076	—	N	—	Murray-Sunset NP	D71345	Z7873	Mus. VIC	−34.7597	141.7758
JEM225	N48	JN627080	—	N	—	Murray-Sunset NP	D71346	Z7872	Mus. VIC	−34.7597	141.7758
JEM226	N12	JN627077	—	N	—	Murray-Sunset NP	D71347	Z7871	Mus. VIC	−34.7597	141.7758
JEM299	N45	JN627044	—	N	—	Hattah NP	D71420	Z7870	Mus. VIC	−34.6853	142.2797
JEM300	N49	JN627100	JN627118	N	—	Hattah NP	D71421	Z7868	Mus. VIC	−34.6853	142.2797
JEM301	N50	JN627098	—	N	—	Hattah NP	D71422	Z7867	Mus. VIC	−34.6853	142.2797
JEM302	N51	JN627096	—	N	—	Hattah NP	D71423	Z7869	Mus. VIC	−34.6853	142.2797
DLE243	N52	JN627039	JN627126	N	—	Rainbow Beach	—	ABTC03912	SA Mus.	−25.9060	153.0790
DLE244	N53	JN627059	—	N	—	Rainbow Beach	—	ABTC03913	SA Mus.	−25.9060	153.0790
DLE245	N53	JN627049	—	N	—	Rainbow Beach	—	ABTC03914	SA Mus.	−25.9060	153.0790
DLE246	N53	JN635333	—	N	—	Rainbow Beach	—	ABTC03915	SA Mus.	−25.9060	153.0790
DLE247	N54	JN627026	—	Y	F	Kroombit Tops	J54855	ABTC24230	QLD Mus.	−24.3667	151.0333
DLE248	N12	JN627060	—	Y	M	N Mulga Stn.	R22791	ABTC53153	SA Mus.	−30.2000	139.7000
DLE249	N55	JN627072	—	Y	M	N Mulga Stn.	R22792	ABTC53154	SA Mus.	−30.2000	139.7000
DLE250	N56	JN627043	—	N	J	Swan Reach CP	R26165	ABTC53191	SA Mus.	−34.6000	139.4833
DLE251	N57	JN627040	—	Y	M	Swan Reach CP	R26902	ABTC53201	SA Mus.	−34.6000	139.4833
DLE252	N12	JN627073	—	Y	M	Arkaroola	R52947	ABTC74088	SA Mus.	−30.1206	139.3986
DLE253	N12	JN627074	—	Y	F	Arkaroola	R52940	ABTC74147	SA Mus.	−30.1206	139.3986

[a] Y, yes; N, no.
[b] M, male; F, female; J, juvenile.
[c] Mt, mountains; Rd., Road, Stn., Station; Tbld., Tablelands.

APPENDIX 2. Registration, sex, species, and locality information for all samples used only for morphological analyses. Coordinates are given in decimal degrees.

Registration no.	Sex[a]	Species	Location[b]	Latitude	Longitude	Museum
2636	F	D. nobbi	Crows Nest	−27.2667	152.0500	Aus. Mus.
11675	F	D. nobbi	Kainkillenbun	−27.1000	151.5333	Aus. Mus.
16955	M	D. nobbi	Cooranga north	−24.7667	151.4000	Aus. Mus.
16959	M	D. nobbi	Bunya Mountains	−26.8500	151.5667	Aus. Mus.
30358	F	D. nobbi	Hillston	−33.4833	145.5333	Aus. Mus.
65949	M	D. nobbi	88 km W Alpha	−23.5667	145.7833	Aus. Mus.
73578	F	D. nobbi	Bathurst	−33.4167	149.5833	Aus. Mus.
74767	M	D. nobbi	4 m S Stanthorpe	−28.7333	141.8667	Aus. Mus.
74768	M	D. nobbi	4 m S Stanthorpe	−28.7333	141.8667	Aus. Mus.
76492	M	D. nobbi	27 km N Albury	−35.9667	147.0167	Aus. Mus.
80246	F	D. nobbi	15 km W Baldry	−32.8167	148.3667	Aus. Mus.
81686	F	D. nobbi	Monoboli NR	−32.2667	150.8833	Aus. Mus.
116024	F	D. nobbi	Melbergen Range	−33.8500	146.0333	Aus. Mus.
130061	M	D. nobbi	26.5 km N Cudgegong River	−32.5667	150.0833	Aus. Mus.
141023	F	D. nobbi	Beulah Stn.	−29.3714	146.2333	Aus. Mus.
141025	M	D. nobbi	Beulah Stn.	−29.3611	146.2242	Aus. Mus.
141585	F	D. nobbi	Kangaroo River SF	−30.1167	152.8333	Aus. Mus.
142078	F	D. nobbi	Beaury SF	−28.5469	152.3364	Aus. Mus.
158578	F	D. nobbi	—	−30.9544	149.5350	Aus. Mus.
161978	F	D. nobbi	Mt Kaputar NP	−30.2375	150.0897	Aus. Mus.
162105	F	D. nobbi	Playgan SF	−30.4464	150.2817	Aus. Mus.
941	F	D. nobbi	Goombungee	−27.5333	151.2833	QLD Mus.
1083	M	D. nobbi	Batavia River	−12.1833	141.9000	QLD Mus.
1084	M	D. nobbi	Batavia River	−12.1833	141.9000	QLD Mus.
10493	M	D. nobbi	Inverell	−29.7667	151.1167	QLD Mus.
10494	M	D. nobbi	Inverell	−29.7667	151.1167	QLD Mus.
30734	F	D. nobbi	Texas Caves	−28.8833	151.4333	QLD Mus.
32346	F	D. nobbi	Boonoo Boonoo Falls	−28.8000	152.1667	QLD Mus.
35150	M	D. nobbi	Airlie Beach	−20.2667	148.7167	QLD Mus.
36887	F	D. nobbi	Epping Forest	−22.3167	146.7500	QLD Mus.
36893	M	D. nobbi	Nine Mile	−23.8333	147.4500	QLD Mus.
37117	F	D. nobbi	Springsure	−24.1333	147.9167	QLD Mus.
38749	M	D. nobbi	Mt Windsor Tbld.	−16.3167	145.0167	QLD Mus.
40123	M	D. nobbi	Kroombit Tops	−24.3667	150.9833	QLD Mus.
42144	M	D. nobbi	Kroombit Tops	−24.3667	150.9833	QLD Mus.
42178	M	D. nobbi	Kroombit Tops	−24.3667	150.9833	QLD Mus.
44358	F	D. nobbi	Victoria Downs North	−20.7167	146.4500	QLD Mus.
44905	M	D. nobbi	Helenslee Stn.	−20.5167	145.7000	QLD Mus.
46702	M	D. nobbi	Myross Stn., 25 km N Aramac	−22.8167	145.3667	QLD Mus.
46723	F	D. nobbi	Winhaven Stn.	−22.9500	145.6833	QLD Mus.
47798	F	D. nobbi	10 km S Barcaldine	−23.6167	145.2833	QLD Mus.
53009	M	D. nobbi	Mt Cleveland	−19.2500	147.0167	QLD Mus.
56060	M	D. nobbi	Ka Ka Mundi NP	−24.8167	147.4000	QLD Mus.
62953	M	D. nobbi	The Bluff, Keysland	−26.2333	151.7000	QLD Mus.
63109	M	D. nobbi	Blair Athol Coal Mine	−22.7000	147.5500	QLD Mus.
64762	F	D. nobbi	Charters Towers	−20.0833	146.2667	QLD Mus.
74745	M	D. nobbi	Bauple SF	−25.8167	152.6167	QLD Mus.
74746	M	D. nobbi	Cunningham's Gap NP, Mt Cordeaux	−28.0333	152.3833	QLD Mus.
75454	M	D. nobbi	Kirrama	−18.1500	145.6167	QLD Mus.
76743	F	D. nobbi	Cudmore NP	−22.9333	146.3667	QLD Mus.
62741	M	D. nobbi	Mt Abbot	−20.1000	147.7500	QLD Mus.
77780	M	D. nobbi	Southward NP	−27.8300	150.1000	QLD Mus.
32596	M	D. phaeospinosa	Blackdown Tbld.	−23.8000	149.1333	QLD Mus.
33335	M	D. phaeospinosa	Blackdown Tbld.	−23.8000	149.0667	QLD Mus.
33336	M	D. phaeospinosa	Blackdown Tbld.	−23.8000	149.0667	QLD Mus.
34294	F	D. phaeospinosa	Blackdown Tbld.	−23.8000	149.1333	QLD Mus.
34295	F	D. phaeospinosa	Blackdown Tbld.	−23.8000	149.1333	QLD Mus.
34296	M	D. phaeospinosa	Blackdown Tbld.	−23.8000	149.1333	QLD Mus.
36891	M	D. phaeospinosa	Blackdown Tbld.	−23.8000	149.1333	QLD Mus.
36892	F	D. phaeospinosa	Reklau Pk.	−23.3333	147.5000	QLD Mus.
38591	F	D. phaeospinosa	Glenhaughton Stn	−25.2333	148.9500	QLD Mus.
50807	F	D. phaeospinosa	Blackdown Tbld.	−23.8000	149.1000	QLD Mus.
28495	J	D. phaeospinosa	Blackdown Tbld.	−23.8000	149.1333	QLD Mus.
30267	J	D. phaeospinosa	Robinson Gorge	−25.2833	149.1500	QLD Mus.
38560	J	D. phaeospinosa	Robinson Gorge	−25.2833	149.1500	QLD Mus.
38590	J	D. phaeospinosa	Robinson Gorge	−25.2833	149.1500	QLD Mus.
36890	F	D. phaeospinosa	Blackdown Tbld.	−23.8000	149.1333	QLD Mus.
38589	J	D. phaeospinosa	Glenhaughton Stn.	−25.2333	148.9500	QLD Mus.

[a] M, male; F, female; J, juvenile.
[b] Pk., peak; Mt, mountains; NP, National Park; Rd., Road, Stn., Station; Tbld., Tablelands.
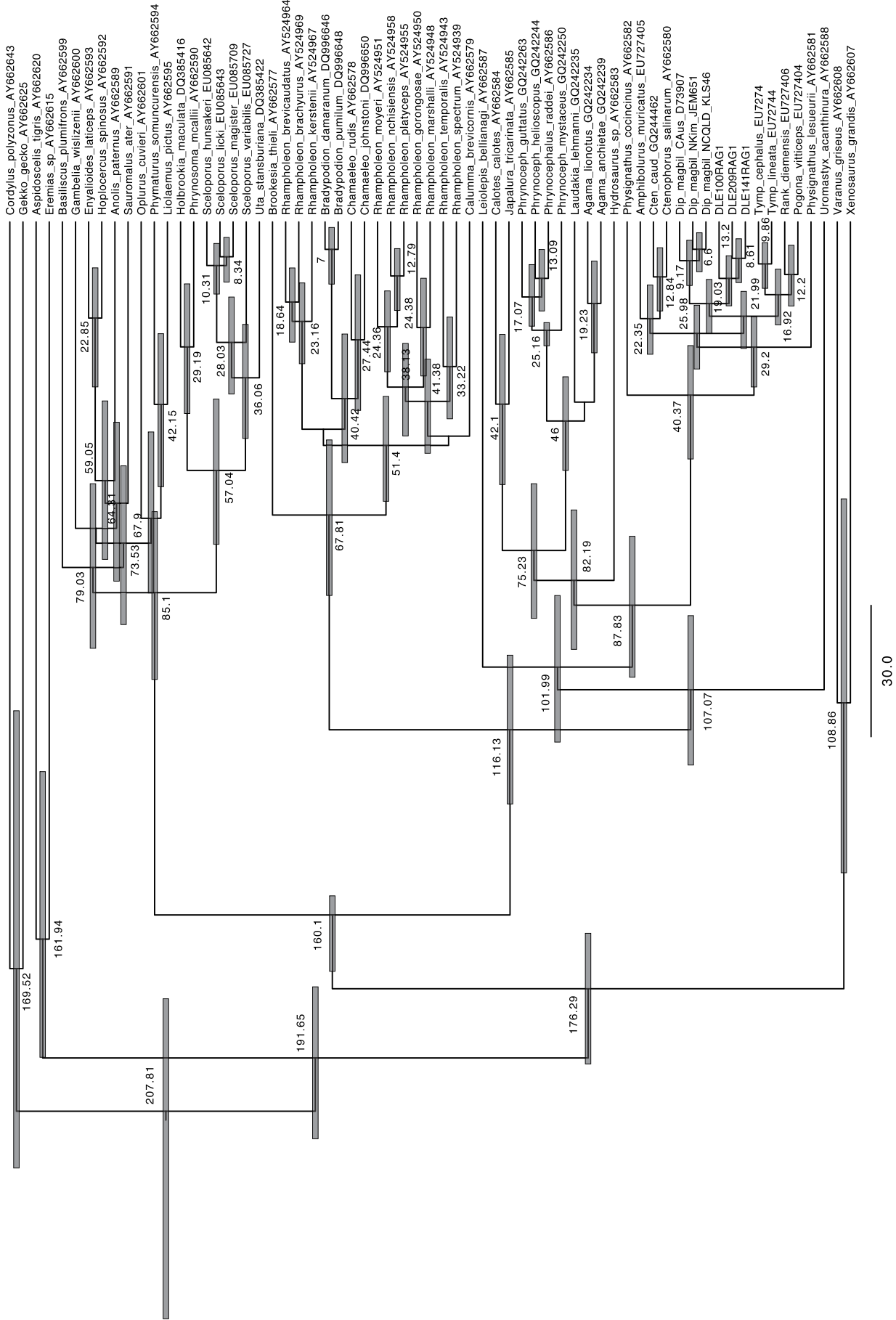
APPENDIX 3. Ultrametric BEAST output tree for the RAG1 analyses. GenBank numbers for sequences are provided. Node ages are shown with bars representing 95% confidence intervals of node ages.

APPENDIX 4. Ultrametric BEAST output for mtDNA analyses. GenBank numbers or registration numbers of specimens are shown. See Appendix 1 for corresponding GenBank numbers for these specimens. Node ages also are shown, with 95% HPD errors around node ages being shaded.